View metadata, citation and similar papers at core.ac.uk

brought to you by CORE

provided by Heriot Watt Pure

Journal of ELECTRONIC MATERIALS, Vol. 47, No. 8, 2018
https://doi.org/10.1007/s11664-018-6372-9
© 2018 The Author(s)

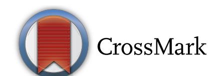

TOPICAL COLLECTION: 18TH INTERNATIONAL CONFERENCE ON II-VI COMPOUNDS

Adhesion Measurements of Epitaxially Lifted MBE-Grown ZnSe

N. MAVRIDI ,[1,2] J. ZHU,[1] N.M. ELDOSE,[1] K.A. PRIOR,[1] and R.T. MOUG[1]

1.—School of Engineering and Physical Sciences, Institute of Photonics and Quantum Sciences (IPAQS), Heriot-Watt University, Edinburgh EH14 4AS, UK. 2.—e-mail: pm24@hw.ac.uk

ZnSe layers grown by molecular beam epitaxy (MBE), after processing by epitaxial lift-off, have been analyzed using fracture mechanics and thin-film interference to determine their adhesion properties on two different substrates, viz. ZnSe and glass, yielding adhesion energy of 270 ± 60 mJ m^{-2} and 34 ± 4 mJ m^{-2}, respectively. These values are considerably larger than if only van der Waals forces were present and imply that adhesion arises from chemical bonding.

Key words: Epitaxial lift-off, II–VI, bonding energy, van der Waals, Se cap, stacking

INTRODUCTION

Current semiconductor fabrication requires devices to be grown on single-crystal substrates, which prevents implementation of some novel device designs due to fundamental material limitations. Epitaxial lift-off (ELO) is a flexible post-growth fabrication technique that overcomes some of these limitations, as it allows an epitaxial layer to be separated from its original substrate and transferred to a new one.[1] Our group has demonstrated this process for II–VI semiconductors using MgS as a sacrificial layer.[2] We have shown that II–VI layers grown on GaAs, InP, and GaP can all be exfoliated using this technique.[3] ELO layers have been successfully transferred to alternative substrates such as glass, laser diodes,[4] distributed Bragg reflectors (DBRs),[5] and $LiNbO_3$.[6] While fabricating these and other devices, it was observed that the adhesion of the lifted layer varied according to the alternative substrate material chosen. Determination of the adhesion energy of II–VI materials on different surfaces could provide better understanding of how to handle and process ELO films.

To date, the methods available to measure the adhesion between two adjacent thin films include tension, shear, and slip tests.[7] These methods have been very successful for macroscopic films, which are durable and easy to handle. However, fragile single-crystal layers are far harder to measure in this way. In this study, we used a fracture mechanics technique and thin-film interference to determine the adhesion coefficient of ZnSe on a new substrate.

(Received January 9, 2018; accepted May 8, 2018; published online May 22, 2018)

FRACTURE MECHANICS

In fracture mechanics it is possible to relate the force required to separate two slabs of material from each other to the adhesion energy holding them together. This method has been used to measure the adhesion energy between thin films,[8,9] as well as to study direct wafer-bonding processes.[10] Here, to measure the adhesion of epitaxially lifted layers on different substrates, we used an adapted version of a double-cantilever system (DCS). The DCS is a stepped structure built of ELO layers deposited on the new substrate, as shown schematically in Fig. 1a.

The adhesion, γ, between the second layer and the substrate is defined by Eq. 1.[11]

$$\gamma = \frac{3}{2}\left(\frac{Et^3h^2}{s^4}\right), \quad (1)$$

where E is the Young's modulus of the drape layer, t is the thickness of the drape layer, h is the step height, and s is the transition region distance. The transition region distance s can be determined from the interference pattern by measuring the distance from the step edge to the edge of the last fringe. Figure 2b shows schematically a plan view of the

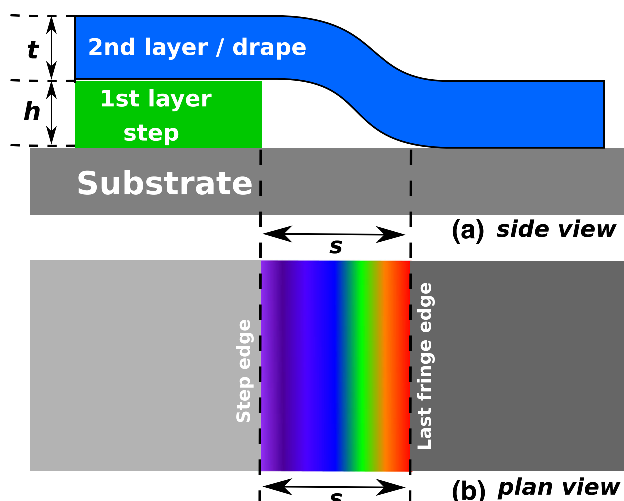

Fig. 1. Schematic diagrams of technique adapted for experimental measurements: (a) side view of DCS and, (b) plan view of DCS as viewed under the microscope. The fringes are generated via thin-film interference between the substrate and drape layer. (Not to scale).

DCS as viewed under an optical microscope. Interference occurs between the substrate and second layer when the thickness of the layers is greater than the wavelength of the microscope light. For this experiment, the DCS was constructed using 1-μm-thick ELO ZnSe layers.

The relationship between the Young's modulus, E, and the stiffness coefficients C_{11} and C_{12} for a cubic crystal is given by Eq. 2:[12]

$$E = \frac{(C_{11} - C_{12}) \times (C_{11} + 2C_{12})}{C_{11} + C_{12}}. \tag{2}$$

For ZnSe, E was calculated to be E = 48 GPa using published stiffness coefficients.[13]

EXPERIMENTAL PROCEDURES

Growth

All structures were grown in a Vacuum Generators V80H molecular beam epitaxy (MBE) system on GaAs(100) substrates following the standard growth procedure.[14] Samples with the structure GaAs (sub)/ZnSe (10 nm)/MgS (7 nm)/ZnSe (1 μm) were grown and subsequently capped with $\sim$ 2 μm of amorphous Se. MgS was used in this structure as a sacrificial layer for subsequent ELO of ZnSe. Flux ratios were set at 1:2 for Zn:Se and 1:36 for Mg:ZnS, corresponding to the optimum growth conditions determined previously.[15] The surface was monitored during growth by reflection high-energy electron diffraction (RHEED). Sharp, streaky c(2×2) and 2×1 RHEED patterns were observed during growth of MgS and ZnSe layers, respectively. After the structure was grown, the substrate temperature was reduced from the growth temperature of 240°C to 30°C with no fluxes applied. During cool-down, the sharp and streaky 2×1 RHEED pattern was maintained, indicative of a flat Se-terminated surface. After cooling, an amorphous Se capping layer was deposited on the ZnSe by exposing the surface to a Se flux of 200 nA beam equivalent pressure (BEP). As soon as Se deposition began, the RHEED patterns changed to amorphous rings, but quickly disappeared for the duration of the deposition. Postgrowth DekTak step profile measurements were used to determine the thickness of the Se cap, and the subsequent deposition rate was found to be $\sim$ 0.5 μm/h. The Se cap was used in this experiment in place of our standard Apiezon W wax carrier[2] as it provided a more flexible carrier for the ELO layer and allowed the top layer of the DCS to drape over the step.

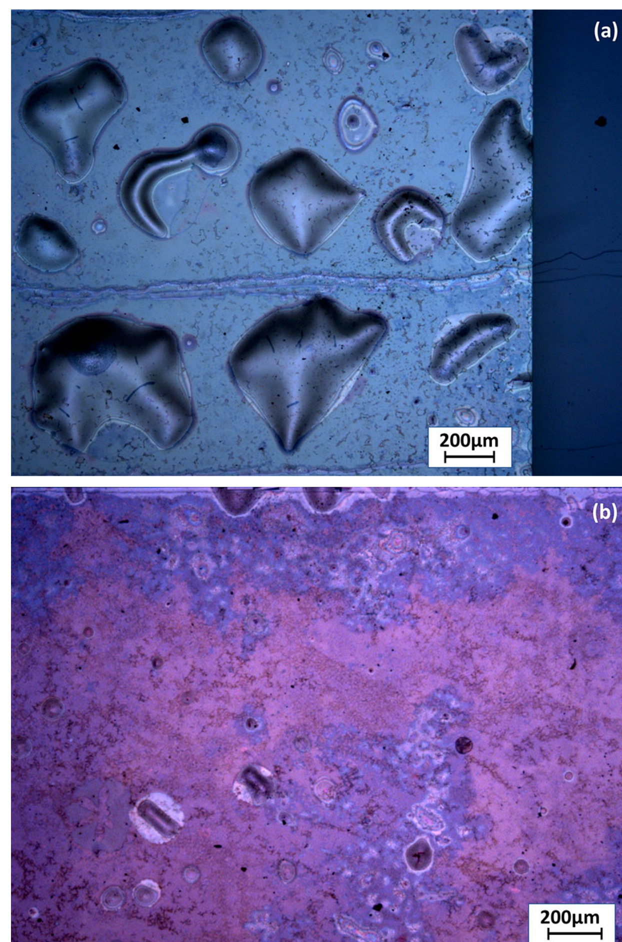

Fig. 2. Microscope images of ZnSe lifted layers deposited on glass after Se cap desorption (black dots are residual Se). Image (a) shows a high density of blisters at the interface, while image (b) shows the significant reduction of blisters after improving the ELO procedure. The difference in color between the images is due to white balance correction in the charge-coupled device (CCD) camera used to collect the images (Color figure online).

Epitaxial Lift-Off

Once removed from the growth chamber, samples were cleaved into square pieces of 10 mm^2, 7 mm^2, and 4 mm^2 to create the desired step structure. The

7 mm^2 piece generates the first step of ZnSe on glass, the 4 mm^2 piece is the second step of ZnSe on ZnSe, and finally the 10 mm^2 was used to drape over both steps to measure the adhesion of ZnSe to ZnSe or glass. Prior to etching, all samples were heated at 100°C for 90 s. It was observed that samples which had not been through this preetch heating process needed several hours (> 24 h) for the ZnSe to be released from the substrate. During this process, the lustre of the Se cap layer changed, from shiny to matte grey. The observed color change in the Se cap layer probably indicates the glass transition from amorphous to polycrystalline Se,[16] which provides a slightly more malleable carrier and allows better etch solution penetration.

The samples were then placed cap side up in a solution of 30% HCl (diluted with H_2O) at room temperature (RT). After the samples were completely etched, separation of the ZnSe layers occurred, with the lifted layer floating at the meniscus, typically within 15 min. Etching the Se-capped samples was observed to be significantly faster than the previously described wax-capped samples, where the etch rate of the MgS sacrificial layer was estimated to be about 3 mm/h.[2,17] This suggests that the tension introduced by the Se cap aids the ELO process in the same way as the wax had previously.[1,2] However, as we can accurately control the thickness of the Se cap, we can tailor the tension applied, giving a higher level of control over the process.

The ZnSe lifted layers were carefully removed from the HCl solution, rinsed in deionized (DI) water, and deposited onto a substrate of borosilicate glass with root-mean-square (RMS) surface roughness of 11 nm, measured using atomic force microscopy (AFM). A small force was applied on the top of the samples to initiate bonding and force the DI water out of the interface. Samples were then left to dry at temperature of 70°C to 100°C for 24 h whilst under light weight of roughly 20 N to 30 N. Once dry, the Se cap was desorbed by gradually heating the samples up to 200°C under atmospheric pressure. Starting from 25°C, the temperature was raised at a rate of 1°C/min until reaching 200°C. The samples were kept at 200°C for 15 min. They were then removed from the hot plate and left to cool down at RT.

Repeating this procedure for all lifted ZnSe layers, two layers were stacked on top of each other to build the step, and subsequently a layer of ZnSe was draped over the step, creating the structure shown in Fig. 1a.

RESULTS AND DISCUSSION

All ELO layers were examined by optical reflection microscopy, and images were taken of the ELO ZnSe layers deposited onto the new substrate, before and after Se cap desorption. Although all the ELO layers adhered well to the glass, initial tests showed a high density of unbonded areas (blisters) from 30 μm to 200 μm across the interface after the Se cap was removed with steep rise in temperature. The sudden temperature change, from 25°C to 200°C, caused expansion of any residual DI water trapped at the interface and formed blisters, as shown in Fig. 2a.

Following this, moderate temperature of 70°C to 100°C was applied to the sample during the 24-h cure period to reduce further the volume of DI water at the interface, and the Se cap was desorbed by gradually heating the samples up to 200°C at a rate of 1°C/min. The slower Se cap desorption did leave some residual Se on the surface (black dots seen in the microscope images in Fig. 2), but it was at low density and judged not to interfere with the measurements. These two modifications of the ELO process significantly reduced the blister density, as shown in Fig. 2b, and provided large enough blister-free areas for subsequent experiments.

The final ZnSe lifted layer of the DCS draped over the step, adopting its shape without breaking or cracking. Using the modified ELO process, expansion of unbound areas was reduced but not completely eliminated, and as a result the unbound area draped over the step did move during the Se desorption.

Interference reflection microscopy was used to measure the transition region distance s, as illustrated in Fig. 1b. Figure 3a shows the fringing between the drape ZnSe layer and the glass substrate, and Fig. 3b shows the fringing between the drape ZnSe layer and the ZnSe. The distance s was determined by measuring the distance from the step edge to the edge of the last fringe, as indicated by arrows in both images of Fig. 3. It can be seen that s varied along the step edge due to some expansion in the void between the glass and the drape layer that lifts the ZnSe off the underlying layer. To correct for this, values of s were measured for many different areas of the sample, and their mean value was used in subsequent calculations with Eq. 1.

The transition region distance s was measured to be 23 ± 4 μm for ZnSe draped onto ZnSe and 38 ± 4 μm for ZnSe draped onto glass. Using Eq. 1, the adhesion energy was calculated to be 270 ± 60 mJ m^{-2} for ZnSe to ZnSe and 34 ± 4 mJ m^{-2} for ZnSe to glass. All the results are listed in Table I. It is important to note that, although the errors here may be large, this is directly related to the s value, which is raised to the fourth power in Eq. 1. In our case, most of the variance in s arises from the expansion along the step edge due to the heating processes. However, the smallest s value measured, and thus the largest adhesion calculated, gives us the upper limit for each case, and is the significant number we are determining.

Using values from literature, the strength of the van der Waals (vdW) force was estimated to be 0.05 mJ m^{-2} and the ZnSe–ZnSe chemical bond strength was calculated to be 400 mJ m^{-2}.[7,8] Our

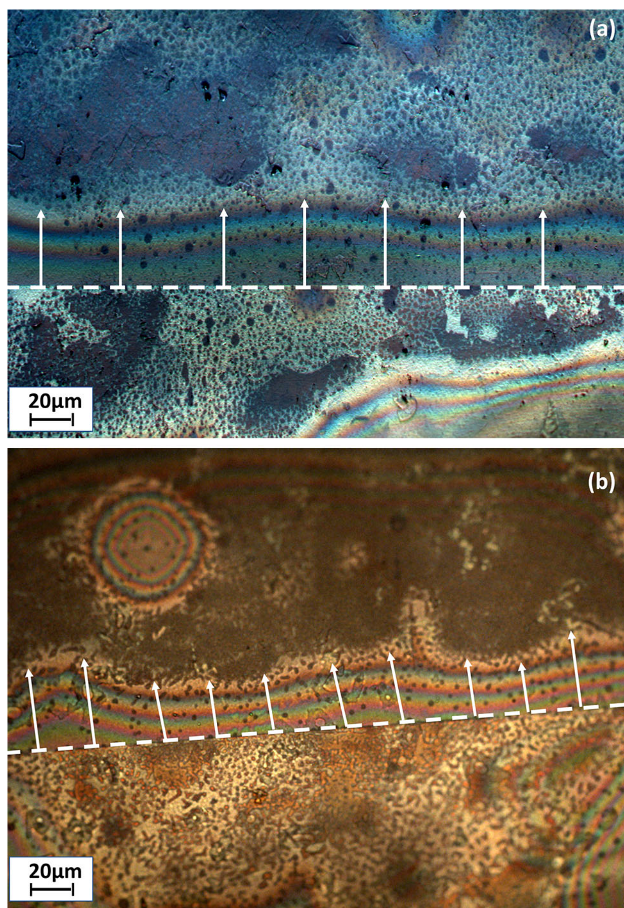

Fig. 3. Microscope images showing interference fringes at the interface between the ZnSe drape layer and (a) glass substrate and (b) ZnSe. The dashed line indicates the edge of the step, and the arrows the transition region distance *s* from the step edge to the edge of the last fringe. Black dots are residual Se (Color figure online).

Table I. Measurements of transition region *s*, and adhesion energy of lifted ZnSe on ZnSe and glass

New substrate	ZnSe	Glass
Transition region distance, s (μm)	23 ± 4	38 ± 4
Adhesion, γ (mJ/m^2)	270 ± 60	34 ± 4

results indicate that the adhesion energies are considerably larger, by several orders of magnitude, than would be expected if only vdW forces were present. The calculated value of 270 ± 60 mJ m^{-2} for adhesion of ZnSe to itself is far beyond the vdW limit and much closer to the value of 400 mJ m^{-2}, indicating that chemical bonding is the main adhesion mechanism. It is likely that slightly weaker chemical bonding is also present in the case of adhesion of ZnSe to glass.

The value of 400 mJ m^{-2} corresponds to the upper limit for chemical bonding between two ZnSe surfaces, where all atomic bonds across the interface between the two layers are restored, creating essentially one perfect crystal. However, in practice, this could not be the case for several reasons:

1. Alignment of the adjacent layers. As no special effort was made to ensure that the crystal axes of the two layers were aligned during ELO, not every Zn (Se) site in the overlayer is aligned with a Se (Zn) site in the layer below. In the case of the amorphous glass layer, the bonds must be Zn–O or Se–O, and no alignment is possible.
2. Lattice matching/strain. Thermally induced strain between the Se cap, the lifted layer, and the new host substrate could lead to uneven bonding and reduce the overall bond strength.
3. Surface roughness. The bonding strength is limited in cases of high surface roughness because the interfacial contact area is restricted to the peaks of the underlying layer while no bonding will occur in the troughs unless the overlayer can deform to follow the contours of the underlying layer. The RMS surface roughness of the glass was measured using AFM to be 11 nm. This is large compared with the grown ZnSe surface with 0.4 nm RMS and may contribute towards reducing the adhesion.
4. Impurity incorporation in bonds. Even in the case of bonding between two ZnSe layers, bonds containing bridging oxygen atoms, such as Zn–O–Zn or Se–O–Se, are expected to form, using oxygen from both the thin oxide layer forming on the surface of the layers and the DI water.

Although the bonding is reduced somewhat from that between two crystal planes, it is still very strong compared with vdW bonding and certainly large enough to enable production of stable multilayer devices. However, the unbonded areas, due to blisters forming at the interface, remain an issue. We believe that the formation of the blisters is a result of trapped DI water at the interface. During Se cap desorption, the samples are heated up to 200°C and any remaining water at the interface expands, forcing the layer away from the substrate, which causes the blisters.

Different approaches must be tested to overcome this problem, changing, for example, layer preparation methods, temperature profiles, and oxide layer formation to determine their effect on the blister size and density. An alternative approach could be to add an annealing step at the ELO process, after Se desorption, and investigate whether this permits closure of the gaps caused by blisters at the interface and thereby increases the bonding strength.

CONCLUSIONS

We demonstrated that fracture mechanics can be adapted to provide a reliable technique to measure the adhesion energy between thin films, monitored using thin-film interference. We successfully built a

DCS using multiple ZnSe layers exfoliated from their substrate and stacked on a new host substrate. The results indicate that the bonding at the interface between ZnSe and ZnSe or glass is predominately chemical instead of van der Waals. Bonding between adjacent layers is not continuous and shows blister-like imperfections, whose density can be reduced if the samples are dried before heating, although the cause of the blisters remains unclear and must be resolved before production of large-area devices. Further investigation and optimization, in terms of the experimental conditions and bonding mechanisms, are essential to improve the reproducibility of this technique as well as its extension to different materials.

OPEN ACCESS

This article is distributed under the terms of the Creative Commons Attribution 4.0 International License (http://creativecommons.org/licenses/by/4.0/), which permits unrestricted use, distribution, and reproduction in any medium, provided you give appropriate credit to the original author(s) and the source, provide a link to the Creative Commons license, and indicate if changes were made.

REFERENCES

1. E. Yablonovitch, T. Gmitter, J. Harbison, and R. Bhat, *Appl. Phys. Lett.* 51, 2222 (2005).
2. A. Balocchi, A. Curran, T.C.M. Graham, C. Bradford, K.A. Prior, and R.J. Warburton, *Appl. Phys. Lett.* 86, 011915 (2005).
3. A. Rajan, I.A. Davidson, R.T. Moug, and K.A. Prior, *J. Appl. Phys.* 114, 243510 (2013).
4. E. Yablonovitch, E. Kapon, T. Gmitter, C. Yun, and R. Bhat, *IEEE Photon Technol. Lett.* 1, 41 (1989).
5. C.D. Yang, C.L. Ho, M.Y. Wu, J.Y. Su, W.J. Ho, and M.C. Wu, *Solid-State Electron.* 47, 1763 (2003).
6. D.A. Fuhrmann, A. Wixforth, R.J. Warburton, J. Ebbecke, A. Curran, J.K. Morrod, and K.A. Prior, *Appl. Phys. Lett.* 94, 193505 (2009).
7. K.L. Mittal, *Electrocomponent. Sci. Technol.* 3, 21 (1976). https://doi.org/10.1155/APEC.3.21.
8. C.A. Finch, *Brit. Poly. J.* 3, 48 (1971).
9. D. Wu, N. Fang, C. Sun, and X. Zhang, *Appl. Phys. Lett.* 81, 3963 (2002).
10. T. Fukushima, H. Hashiguchi, H. Yonekura, H. Kino, M. Murugesan, J.C. Bea, K.W. Lee, T. Tanaka, and M. Koyanagi, *Micromachines* (2016). https://doi.org/10.3390/mi7100184.
11. M.P. de Boer and T. Michalske, *J. Appl. Phys.* 86, 817 (1999). https://doi.org/10.1063/1.370809.
12. A. Kelly, G.W. Groves, and P. Kidd, *Crystallography and Crystal Defects*, 2nd ed. (England: Wiley, 2000), pp. 164–172.
13. C.G. Hodgins and J.C. Irwin, *Phys. Stat. Sol. (a)* 28, 647 (1975).
14. A. Rajan, R.T. Moug, and K.A. Prior, *Appl. Phys. Lett.* 102, 032102 (2013).
15. A. Rajan, R.T. Moug, and K.A. Prior, *Semicond. Sci. Technol.* 29, 025006 (2014).
16. J.C. Mauro and R.J. Loucks, *Phys. Rev. B* 76, 174202 (2007).
17. A. Curran, S. Brown, R.J. Warburton, and K.A. Prior, *Phys. Status Solidi B* 247, 1399 (2010).